

Measurement of the Deformation and Adhesion of Rough Solids in Contact

R. A. Quon,[†] R. F. Knarr,[†] and T. K. Vanderlick^{*‡}

Department of Chemical Engineering, University of Pennsylvania, Philadelphia, Pennsylvania 19104, and
Department of Chemical Engineering, Princeton University, Princeton, New Jersey 08544

Received: February 9, 1999; In Final Form: April 26, 1999

A contact mechanics approach is used to study the impact of deformations on the adhesion between microscopically rough gold and molecularly smooth mica. The surface forces apparatus was used to directly measure deformations at the interface and in the bulk, while also controlling applied loads. Surface forces and applied loads act to deform gold asperities in an unrecoverable fashion. Concurrent bulk deformations, namely the nominal area of contact, are also nonreversible. Using Johnson–Kendall–Roberts theory to interpret these findings illustrates how adhesion between the bodies effectively increases with increasing load. Correlating this phenomenon to deformations at the interface details how adhesion varies when multiple metallic asperities contact and deform under external stress. Moreover, observed hysteresis is explained.

Introduction

An understanding of adhesion between solid bodies is important to many fields of science and technology, including lubrication, solids handling, and surface micromachining. Fundamental to this phenomenon is the action of van der Waals forces between solids. At sufficient proximity, these ubiquitous forces serve to drive bodies together and maintain them in contact. While van der Waals forces govern the phenomenon of adhesion, their actions are often better understood, experimentally, in terms of interfacial free energies.¹

Bringing two surfaces together into intimate contact to form an interface is often defined by a work of adhesion, and is related to thermodynamic interfacial free energies by the Dupré equation:

$$W = \gamma_1 + \gamma_2 - \gamma_{12} \quad (1)$$

where the surface free energies of materials 1 and 2 are represented by γ_1 and γ_2 respectively, and γ_{12} is the interfacial free energy between materials 1 and 2. In other words, the work of adhesion is the net free energy change associated with creating new material interfaces. “Work” in this context is not path dependent and does not consider the work associated with mechanical deformations of contacting solids.

Measurement of this work of adhesion even between smooth, elastic solids must consider contact mechanics, which describe the deformation of contacting solids due to internal or external stresses. Theory for this ideal case, as developed by Johnson, Kendall, and Roberts (JKR), describes the deformation of two contacting solid spheres due to the applied load and adhesion between the surfaces.² JKR tested their model by measuring the deformation and adhesion of soft rubber spheres in contact and found very good agreement with their theory.

The work of adhesion is a useful concept, but an impractical measure.³ The idea of doing work to separate an interface makes intuitive sense. Contact, however, is rarely intimate over any useful engineering dimension, even for microelectromechanical

systems (MEMS) and devices. Simply put, engineering surfaces are rough; contact is limited to asperities protruding from the surfaces.⁴ Nonintimate contact can still result in adhesive contact, yet not yield a true work of adhesion since van der Waals interactions depend critically on the separation between the two surfaces.⁵

Whether two surfaces stick together is not solely determined by the net attraction between molecules. Bodies of different geometry (e.g. sphere and flat, or two crossed cylinders) will deform macroscopically in response to being placed into contact. Bulk contact geometry as well as material properties, such as the elastic modulus and hardness, all affect the conformity of one surface to another, and must also be considered when separating two adhering solids.

Unfortunately, contact mechanics theory for rough, adhesive surfaces is of limited practical use to experimentalists and engineers. The models do show how adhesive forces vary as a function of surface separation.^{6,7} Bridging these theoretical treatments to experiment is, however, difficult. Models have only considered contact between parallel, flat plates, which are experimentally impractical due to edge effects and alignment problems. Further, certain model variables are difficult to measure, most notably the separation between contacting surfaces.

Most investigators avoid the complications of roughness, preferring to study the contact between soft elastic solids, where JKR theory is applicable,^{8,9} or to study van der Waals interactions between rigid, smooth mica.^{10,11} Extensive studies on the contact and adherence of metals have been conducted, but roughness was not considered.^{12–14} In fact, much of our experimental understanding on how roughness affects adhesion follows from the work by Tabor and co-workers of nearly 25 years ago.^{15–17}

Recently, Levins et al. investigated the adhesion of metallic, multiasperity contacts using the surface forces apparatus (SFA),^{4,18} a device well-established for measuring the forces between, and associated deformations of, two curved surfaces in contact.^{11,19,20} Central to this force measuring technique is the use of multiple beam interferometry (MBI) to determine the separation between surfaces.²¹ By selecting one of the interferometric mirrors to double as an experimental surface,

* To whom correspondence should be addressed.

[†] University of Pennsylvania.

[‡] Princeton University.

detailed studies of metallic, multisasperity contacts can be made. This method offers the unique ability to directly measure deformations of both the bulk geometry and interfacial microstructure concurrently.

Using this powerful method, Levins et al.¹⁸ examined contact between optically smooth metals (silver, gold) and molecularly smooth mica. The metal, though optically smooth, is still rough on the nanometer level. Their studies showed that surface forces alone are sufficient to induce changes in microstructure. Deformations occur immediately upon contact, and continue until sufficient material can balance the natural load exerted by the surface forces. He further showed how adhesion scales with his optical measure of surface roughness determined under the condition of no applied loads.²²

This paper extends the study of the adhesive behavior between rough surfaces by experimentally measuring contact deformations, including the separation between solids at the interface, with applied loads. For this study, contact between a thermally evaporated thin gold film and molecularly smooth mica is considered. This contact mechanics approach allows us to characterize the "effective" adhesion of the interface so comparisons of two different systems, or even different experiments on the same system, can be made. Furthermore, we demonstrate how this effective adhesion and changes to the microstructure at the interface are related, thus bridging experiment to theory.

Background on Contact Mechanics

The contact mechanics approach has its origins with Hertz, who, in 1881, considered the case of two nonadhering spheres.²³ His approach determines how the contact area and stress distribution between two perfectly elastic, smooth spheres varies with an applied normal load. Under no load, the two solids contact at a point and can freely separate.

Johnson, Kendall, and Roberts extended this approach 90 years later to smooth, elastic spheres in adhesive contact.² Adhesion between the solids results from each surface possessing a finite surface free energy. Thus, under no load, the two solids contact with a finite area; the energy of the adhesive bond is absorbed by the elastic properties of the material. The balance of an applied load with the adhesive and elastic forces of the contacting solids results in the following equation:

$$a^3 = \frac{R}{K} [P + 3\pi RW + \sqrt{6\pi RWP + (3\pi RW)^2}] \quad (2)$$

The equation relates variation of the radius of contact, a , with applied load, P , and the Dupre work of adhesion, W . Bulk deformation is also affected by the elastic constant, K , of the system as well as the radius of curvature, R . The theory also predicts the force needed to separate the adhesive bodies,

$$P_s = -1.5\pi RW \quad (3)$$

where P_s is commonly known as the separation, or pull-off, force.

As illustrated in Figure 1, the initial contact radius under no load increases as the work of adhesion between the surfaces increases for a given radius of curvature and elastic constant for the system. Simply put, more of the solid must deform to balance the attractive force exerted between the surfaces. JKR theory is appealing to the experimentalist since the variables are either measured or controlled.

Simulating the contact mechanics of rough surfaces is complicated even in the limiting case where no attractive forces exist. The first treatment of this problem considered a flat plate

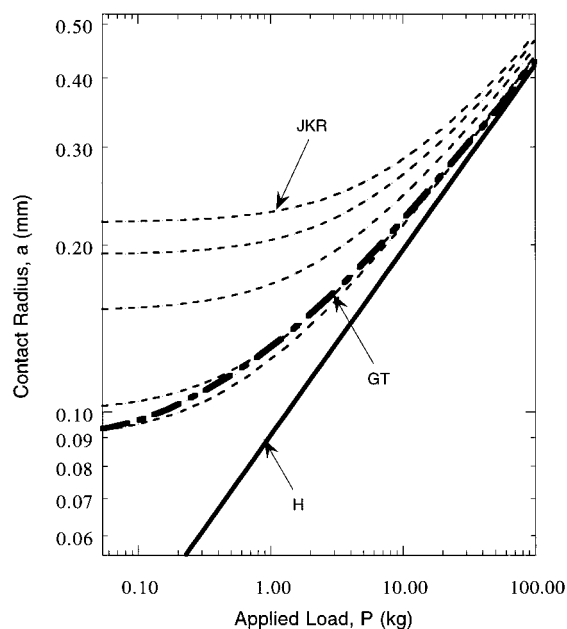


Figure 1. Theoretical determinations of contact between a flat plate and a sphere with radius of 10 mm for a system with an elastic constant of 13333.3 kg/mm². The curve labeled as H (heavy line) describes nonadhesive contact between smooth surfaces, as determined by Hertz. The curve labeled as GT (heavy, dash-dotted line) describes nonadhesive contact between rough surfaces, as determined by Greenwood and Tripp. The contact mechanics curve predicted by Greenwood and Tripp corresponds to a root-mean-square surface roughness of 0.5 μ m. The curves labeled as JKR (light dashed lines) describe adhesive contact between smooth surfaces, as determined by Johnson-Kendall-Roberts. The curves representing the JKR theory possess various values of work of adhesion, from 0.0051 J/m² (the dashed line with the smallest initial contact radius) to 0.075 J/m² (the dashed line with the largest initial contact radius).

geometry.²⁴ This seminal work by Greenwood and Williamson illustrated the dependence of asperity deformation on the surface statistics. The statistical distribution of these asperities defines the roughness and determines the extent of contact deformation between the solids. The statistical basis of the roughness allows the modeling of contact by considering one of the surfaces to be smooth and the other rough, which with proper averaging is shown to be equivalent.

While contact theory is well-developed for smooth spherical solids, to our knowledge only one model considering roughness and this geometry exists. Moreover, this study examined the limited case of nonadhering, perfectly elastic solids.²⁵ The model accounts for changes in the bulk geometry, as reflected in a changing contact area, and at the interface, as reflected in the deformation of contacting asperities. One of the surprising findings from this study is that the roughness of the surface effectively yields a finite contact area when the surfaces are brought together under negligible load, which is in contrast to the Hertzian solution where nonadhesive spheres contact at a point; there is no finite contact area. The effective initial contact area is well-approximated by

$$a = \sqrt{2R\sigma} \quad (4)$$

where a is the effective contact radius, R is the bulk radius of curvature of the system, and σ is the root-mean-square roughness of the surface asperities. In reality, contact initially occurs at the point of the highest asperity. The tiniest load, however, will deform the asperity, quickly resulting in more asperity contacts over the surface. Thus, an apparent contact radius is observed at negligible loads.

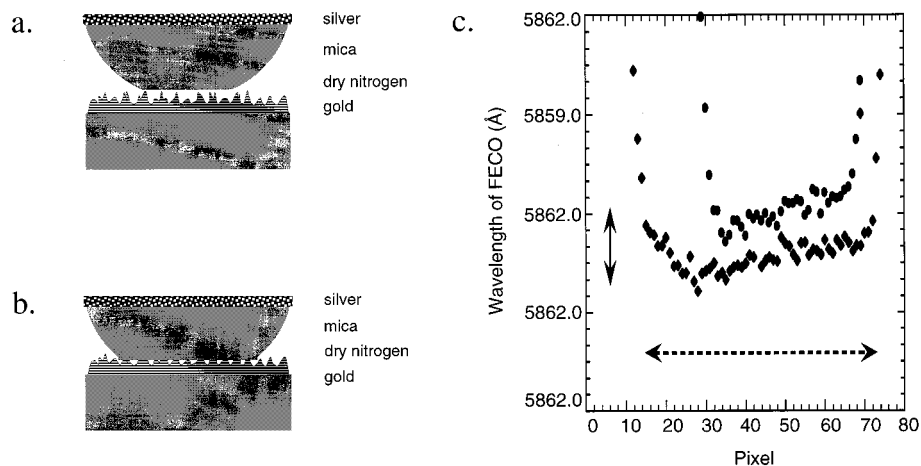


Figure 2. Schematics illustrate how experimental surfaces contact in the SFA. The shape and position of fringes of equal chromatic order (FECO), representing the contacting solids, change due to applied loads and surface forces. (A) Schematic representing the interference filter corresponding to surfaces in contact under 0.0075 N of applied load. (B) Schematic representing the interference filter corresponding to surfaces in contact under 0.051 N of applied load. (C) Filled diamonds represent FECO where a 0.0075 N external load is applied. Filled circles represent FECO where a 0.051 N external load is applied. The solid line highlights the change in FECO position (i.e., roughness) due to the applied load. The dashed line illustrates how contact diameters are measured.

Distinguishing between rough, nonadhesive contact and smooth, adhesive contact could be difficult, as we demonstrate in Figure 1. The growth of the contact area due to an applied load for a rough, nonadhering sphere against a flat surface is not distinctly different from the loading behavior of smooth bodies in adhesive contact with the same bulk geometry.

Experimental Method

These contact mechanics studies use a SFA which is identical to ones described in detail elsewhere.^{20,26} This surface forces balance technique works in conjunction with multiple beam interferometry (MBI),²¹ and thus the experimental surfaces are part of an interference filter. For the case studied here, the experimental surfaces are rough gold in contact with smooth mica.

The interference filter used in this study includes two thin and uniformly thick mica sheets, cleaved so that the surfaces are smooth on a molecular scale. The sheets are then coated on one side with a thin metal film—one sheet with gold and the other with silver. The sheets are glued to cylindrical quartz supports so that on one substrate the gold film is exposed, while on the other, the silver-side is down, leaving mica exposed. The cylinders are then mounted in the SFA at right angles, with the mica surface opposite the gold surface. The interference filter has the final form of silver/mica/intervening medium/gold, as illustrated in Figure 2A,B. The medium in this study is dry nitrogen.

The construction of the interference filter for these experiments allows us to directly measure deformations in both the bulk geometry and interfacial microstructure concurrently. Characterization of the rough metal interface is described in detail by Levins et al.^{22,27} Salient features of this method, as it applies to this study, are summarized below. More details can be found in the Supporting Information.

A. Measurement of Deformations at the Interface. Contact between the rough gold film and smooth mica is not intimate; air is trapped between contacting asperities. The sensitivity of MBI to this trapped dielectric is the key to characterizing roughness at the interface. Comparison of interferometric spectra of our experimental filter with a calibration filter, one in which no trapped dielectric exists, yields a spectral shift that is a measure of roughness.²⁸

Translations of this absolute measure of nonintimacy to standard definitions of roughness are, however, qualitative at

best. Inherent measurement error in the SFA technique and modeling error in the characterization of roughness make quantitative relationships between roughness measures from the SFA and, say, an atomic force microscope (AFM) difficult. Measurement error of absolute roughness, as detailed in the Supporting Information, is up to 40 Å. It is important to realize that these sources of uncertainty do not limit one's ability to monitor and measure changes of roughness within a filter because of the high precision of MBI. As a general rule of thumb (verifiable by calculation), for a given model of topography, spectra shifting to longer wavelengths varies linearly with the characteristic length of roughness.²⁹ Changes in deformations are important in these contact mechanics studies.

B. Measurement of Deformations in the Bulk. The surfaces placed in the force apparatus are curved, so the gap between them is not uniform. MBI captures the relative configuration of the opposing surfaces at their nearest approach. In other words, MBI can also be used to measure the deformation of the surfaces about the contact region as a function of applied load.¹¹ Figure 2C illustrates how a series of both bulk and interfacial deformations are captured using MBI as a function of load. The flattened area represents the nominal area of contact. As applied loads increase, the flat region grows, or deforms, in response. The figure also shows a shift of the spectral pattern to shorter wavelengths, suggesting that gold asperities in contact with the mica are deforming with a resultant decrease in the effective thickness of the trapped dielectric. For a perfectly intimate interface, such as when two mica sheets contact, no shift of the spectral patterns to shorter wavelengths is ever observed.

C. Experimental Design. Design of our experiments must consider the dynamics noted by Levins et al.¹⁸ His experiments showed how rough metal films deform against mica under no external loads over time, as determined by changes in the position of interferometric spectra. Our studies required us to characterize the time dependent nature of this phenomenon, as we illustrate in Figure 3. This deformation proceeds over time in an exponential fashion. For contact between rough gold and mica, a typical time constant for this phenomenon is on the order of hundreds of minutes.

Continuous application of an applied load at a sufficient rate lessens the effect of this natural relaxation. In addition, control

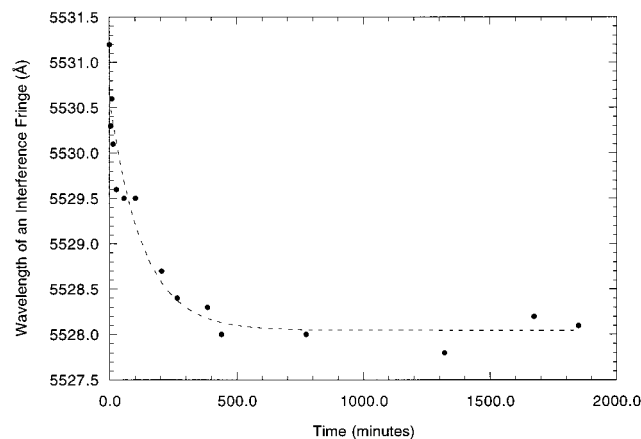


Figure 3. Gold asperities deform against mica under the action of surface forces over time. The change of the transmitted spectra to shorter wavelengths represents a reduction in roughness. The time constant for this relaxation is 130 min.

of the applied force allows us to account for the external load, P , in the JKR equation for our analysis. To this end, a rate of $7.6 \mu\text{N}$ per second was steadily applied while loading and unloading the surfaces in all experiments and was controlled by a microstepper controller (Compumotor, AT-6400). Compressive loads of up to 0.05 N were reached before retracting the surfaces back to zero load; whereupon, tensile loads were applied until the surfaces jumped apart. The deflection of the spring at the moment of separation is very nearly equal to the separation of the surfaces after the jump, as determined by multiple beam interferometry. The strength of adhesion, or the “pull-off” force, P_s , is simply equal to the deflection of the spring multiplied by the spring constant. This pull-off force can be related to the work of adhesion as determined by JKR theory.

Preparation and Characterization of Surfaces. Muscovite mica was cleaved into thin sheets, approximately $3\text{--}4 \mu\text{m}$, of uniform thickness. Squares of mica (typically 1 cm^2) were then cut from this sheet and placed on two large support plates of freshly cleaved mica.³⁰

A thin silver film was thermally evaporated onto one of the support plates from a tungsten boat in a turbo-pumped Pyrex bell-jar system, thus covering the exposed faces of the mica sheets. Evaporation rates and final film thicknesses were measured using a quartz crystal monitor. The source metal was 99.999% pure. Base pressure during the evaporation was better than 8×10^{-7} Torr. Rates of evaporation for silver ranged between 3.5 and 4.0 \AA/s . Film thickness was approximately 500 \AA . One of the silvered mica sheets was removed and glued to a cylindrical quartz disk using epoxy resin Epon 1004 (Shell), with the metal side against the resin and the bare mica surface exposed. The disk was then affixed in the SFA on the upper rigid mount.

The lower surface was prepared by gluing a bare mica sheet from the other support plate to another cylindrical quartz disk, whereupon the disk was placed in the evaporation chamber and a thin gold film of 500 \AA thickness was deposited onto the mica surface. Gold of 99.999% purity was thermally evaporated at a rate of 2.5 \AA/s under a base pressure of better than 8×10^{-7} Torr. Our facility allows up to two disks to be coated simultaneously; thus, two gold films are formed under the exact same conditions. This batch preparation allows us to compare the contact mechanics between near identical surfaces, as well as between different evaporations.

A gold-coated disk was then mounted to the leaf-spring, opposite the bare mica surface, in the SFA. Thus, the interfer-

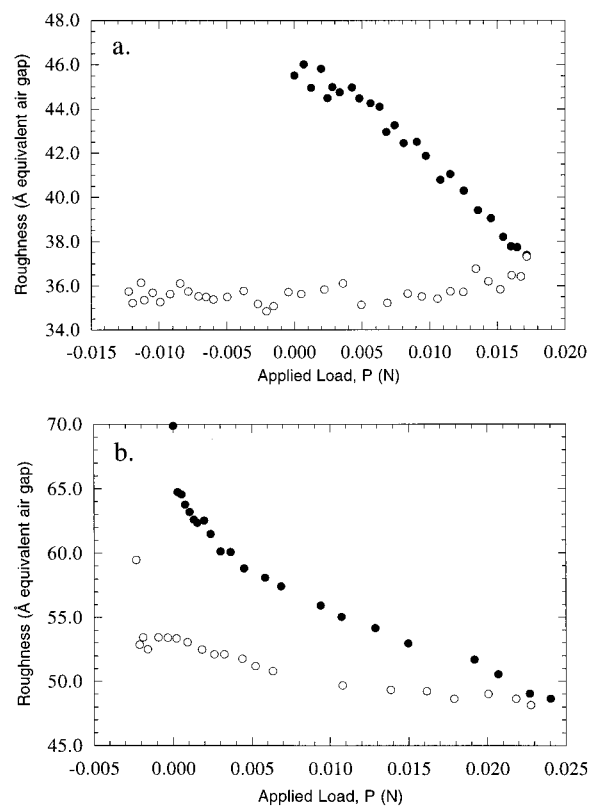


Figure 4. Roughness changes with applied loads. Filled circles represent the loading cycle while open circles represent the unloading cycle. (A) Deformations represent a system where R is 0.020 m and K is 25 GPa . (b) Observed deformations represent a family of surfaces different than ones used for panel a. R is 0.0173 m and K is 19 GPa .

ometer was constructed. The final step prior to experimentation involved sealing the SFA with a small vial of desiccant and then purging with nitrogen gas for at least 0.5 h .

The topography of many rough surfaces can be characterized as a Gaussian distribution of asperities.³¹ Our metallic films of thermally evaporated gold are well-described by this model. This distribution is commonly described by its root-mean-square (the rms roughness), the density of asperity peaks, and the average radius of curvature of an asperity. An experimental rule of thumb shows the product of these three parameters to be 0.05 .¹⁵ Greenwood and Williamson demonstrated the importance of these three parameters to the way in which surfaces contact and deform.²⁴ Improved methods of profilometry such as atomic force microscopy (AFM) allow us to determine these parameters directly. Analysis by our AFM facility shows gold films prepared in the manner above have an rms roughness of 19 \AA and a density of $2600 \text{ peaks}/\mu\text{m}^2$. The radius of curvature of the asperities is estimated to fall between 60 and 100 \AA . These values are consistent with the analysis of other experimenters.²²

Results and Discussion

Two types of deformations occur when a rough body contacts mica: one at the interface (microdeformations) and the other in the bulk geometry (macrodeformations). For ease of understanding, these observations are presented separately, then jointly discussed.

With regard to microdeformations, surface forces and applied loads deform gold asperities plastically, reducing roughness, as Figure 4A,B illustrates. Deformations are not recoverable, a feature common to all experiments in this study. Both elastic and plastic deformations of the contacting asperities occur,

whether one mode dominates, however, depends on the topography and material properties of the surfaces involved. Prediction of the deformation mode is simply determined by a plasticity index, $\Psi = (E/H)(\sigma/\beta)^{0.5}$, introduced by Greenwood and Williamson.²⁴ Here, H is the hardness of the asperities, E is the elastic modulus of the contacting materials, σ is the root-mean-square roughness, and β is the average radius of curvature of a contacting asperity. Values greater than 1 imply that contacting asperities will flow plastically. For gold, the softer material, against mica, the hardness is about 10^9 N/m² and the elastic modulus is 50×10^9 N/m²; using values reported above for the other parameters, we find $\Psi = 24$. Such a high plasticity index is consistent with the direct observation reported herein.

Even though contact between rough gold and smooth mica is the only system considered here, the deformation behavior among experiments is not identical. Close inspection of the deformation behavior reveals subtle differences, particularly when applied loads are relieved. Figure 4A shows no recovery of the deformation. On the other hand, Figure 4B shows a slight, but steady, recovery of the deformation just prior to separation of the surfaces. At this point, a sharp recovery is observed. We have observed similar behavior when surface forces alone act (i.e., in the absence of external loads). The gold surface used to produce Figure 4A comes from a different batch (evaporation) than those tested for Figure 4B.

The difference in behavior between batches may be attributed to the difficulty in preparing surfaces with consistent surface energy, especially when experiments cannot be performed in ultrahigh vacuum. For instance, many studies on the adhesion between mica surfaces are in disagreement, even when using a similar experimental apparatus,^{10,11,32} defining a unique surface energy for mica is difficult.¹⁰ So, our observations are not surprising nor unexpected. The uncertainty in the interfacial energies of the contacting surfaces does not, however, affect the roughness statistics. Differences in deformation behavior may also result from variations in bulk and/or surface mechanical properties arising from the stochastic nature of these polycrystalline gold films.

The remarkable consistency in deformation behavior between surfaces from within the same batch is noteworthy. As in Figure 4A, no recovery of asperity deformation is observed for the twin surface created during the same evaporation. The similarity in behavior for a batch of surfaces is also reproduced for changes in bulk geometry.

Deformation of asperities at the interface is accompanied by deformations of the bulk geometry, as captured by the shape of the fringes of equal chromatic order (FECO). As the contact of crossed cylinders is similar to contact between a sphere and a flat plate, the flat region of the FECO reasonably estimates the diameter of a circular contact area. Monitoring the changes of this contact diameter with applied loads permits us to relate our observations to classical theories of contact by Hertz and JKR.

Parts A and B of Figure 5 illustrate the changes in bulk geometry, in terms of dimensionless contact radius versus the dimensionless applied load, corresponding to the microdeformation shown respectively in parts A and B of Figure 4. Direct experimental measurement of the macrocontact behavior between rough gold and smooth mica is represented by the solid and open circles. Contact behavior between ideally smooth bodies of similar elastic properties and bulk geometry, but with different interfacial works of adhesion, is represented by the solid lines; the lines are theoretical curves calculated from JKR theory. As is readily seen, the changes in bulk geometry with applied compressive loads do not trace any curve determined

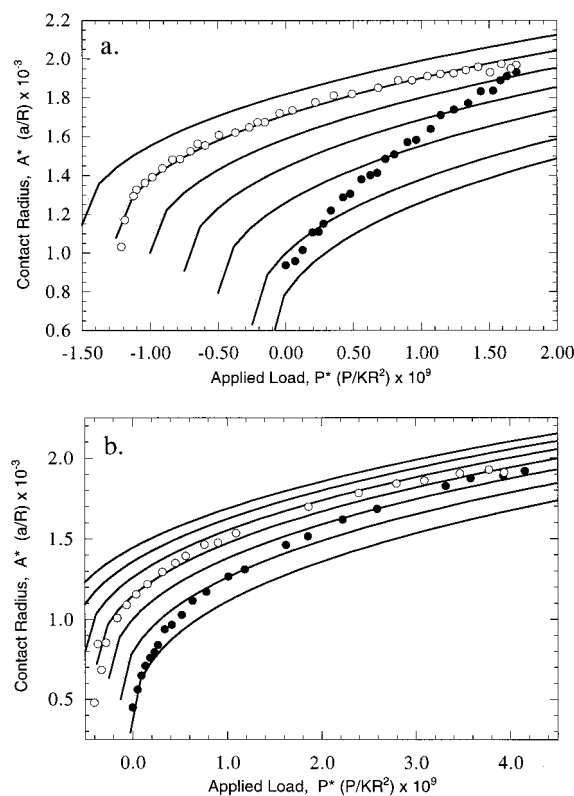


Figure 5. Contact mechanics of a rough gold film against smooth mica in dimensionless variables. Filled circles represent the loading cycle while open circles represent the unloading cycle. The solid lines represent theoretical behavior predicted by JKR. (A) R is 0.020 m and K is 25 GPa. For the theoretical curves predicted by JKR, W^* ($3\pi W_{ad}/KR \times 10^{-9}$) changes for each line. From bottom to top, W^* is 0.25, 0.50, 1.00, 1.50, 2.00, 2.50, and 3.00. (B) R is 0.0173 m and K is 19 GPa. W^* is, from bottom to top, 0.05, 0.25, 0.50, 0.75, 1.00, 1.25, and 1.50.

from JKR theory. Instead, the behavior crosses many curves of constant work of adhesion. In fact, the work of adhesion appears to effectively increase with increasing loads. On the other hand, the separation process closely follows a path of constant work of adhesion.

Relief of the applied stress on the surfaces demonstrates the irreversible nature of the contact mechanics, as is clearly seen in Figure 5A,B. Further, a finite tensile load is required to separate the two bodies; contact is clearly adhesive. Figure 5A is interesting since the unloading behavior traces a theoretical JKR curve quite well. The good fit to theory allows us to reasonably estimate the elastic constant for the system as well as a work of adhesion from eq 2, as detailed in the Supporting Information. For this experiment, JKR theory predicts a pull-off force of 627 mN/m; the direct measure of the pull-off force is 612 mN/m, a difference of 2%. Measures of the pull-off force between surfaces prepared in the same batch as those shown in Figure 5A also differ by less than 3%, and JKR theory is a good predictor of unloading behavior. Again, similarities in behavior are noted within a batch of surfaces.

The observed macrodeformations suggest that adhesion increases with increasing compressive loads, while remaining nearly invariant during separation. This notion is best understood in terms of an effective work of adhesion, which differs from the fundamental work of adhesion in the Dupre equation. The effective work of adhesion between rough surfaces is simply defined as the work of adhesion between smooth surfaces for an equivalent bulk deformation, as determined from JKR theory. So, for a given elastic constant and radius of curvature, an

effective work of adhesion can be calculated from JKR theory with respect to the applied load and measured radius of contact. This intuitive concept is useful in the analysis of our experimental studies as the fundamental work of adhesion between our two surfaces cannot be known a priori for reasons stated earlier.

Comparison of the two deformation behaviors, at the interface and in the bulk, leads us to the observation that the effective work of adhesion is a function of the measured roughness. Figure 4A shows how the roughness, or average separation between the contacting surfaces, remains invariant while applied loads are removed. While the separation remains constant, the bulk deforms in a manner consistent with JKR theory, as shown in Figure 5A. Similar behavior is demonstrated in Figures 4B and 5B. Figure 4B shows the recovery of deformations in a slight and steady fashion until just prior to separation, when a sharp recovery of deformation is observed. Likewise in Figure 5B, upon retreat of the surfaces, the bulk deforms in a manner consistent with a slight, but steady, decrease in the effective work of adhesion until just prior to separation. We thus assert that interfacial deformations are coupled to the measure of an effective work of adhesion. Furthermore, we can interpret the contact between rough adhesive bodies in terms of the contact mechanics theory developed by JKR.

Use of JKR theory allows us to isolate the relation between adhesion and separation of the surfaces, due to roughness, by simply showing how the effective work of adhesion varies with roughness. In other words, the macrodeformation at a particular load corresponds to a unique effective work of adhesion, which in turn corresponds to a microdeformation. Thus, a relation between adhesion and surface separation is newly revealed, as illustrated by Figure 6A,B. The concept of an effective work of adhesion is used to recast our direct measurements of deformations at the interface and in the bulk to illuminate how adhesion changes between rough solids in a contact mechanics experiment.

Reporting the pull-off force as a measure of the strength of adhesion is convenient for comparison with actual measures of pull-off force. For instance, Levins et al.²² report pull-off force as a function of roughness, but their measures do not specifically account for the deformation of asperities in the separation process; Knarr et al.⁵ present such measurements for even smoother gold/mica interfaces. For this reason, we choose to report the strength of adhesion not in terms of the effective work of adhesion, as defined above, but rather as an effective pull-off force as related to the former through eq 3. Note that this measure of adhesion is not associated with an actual separation event. Effective pull-off force versus roughness is shown by Figure 6A,B.

Figure 6A demonstrates this relation for contacts on two different surfaces within the same batch, one of which corresponds to the deformations observed in Figures 4A and 5A. The most striking observation is the similarity of the trends between the two experiments. In both instances, the pull-off force decreases by 44 N/m per Å decrease in surface separation; compressive forces of roughly 0.017 N were applied before the surfaces were unloaded in each case. One might expect our trends to overlay since Chang et al.⁶ has theoretically shown how adherence force (an alternate measure of adhesive strength) is a function of relative separation for a given roughness statistic and fundamental work of adhesion. Our ability to measure an absolute roughness (surface separation) is, however, limited, so the result is not too disconcerting. Sliding the trends along the abscissa so that they overlap, as illustrated by the inset of Figure

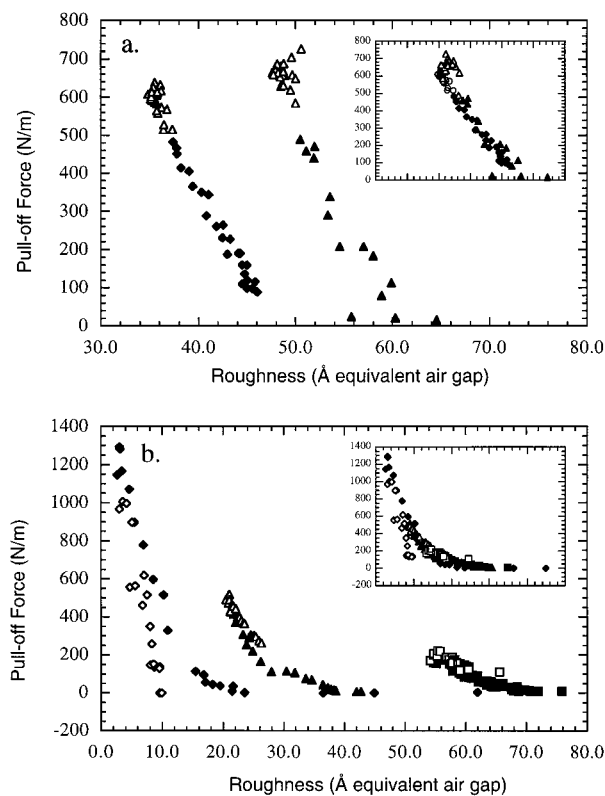


Figure 6. Change in the effective adhesion, reported as a pull-off force, P_s , as a function of roughness during a contact mechanics experiment. (A) Filled diamonds represent a system where R is 0.020 m, K is 25 GPa, and maximum applied load, ΔP , is 0.017 N. Filled triangles represent a system where R is 0.0123 m, K is 25 GPa, and ΔP is 0.016 N. (B) Filled diamonds represent a system where R is 0.0134 m, K is 31 GPa, and ΔP is 0.045 N. Filled triangles represent a system where R is 0.0186 m, K is 27 GPa, and ΔP is 0.032 N. Filled squares represent a system where R is 0.0173 m, K is 19 GPa, and ΔP is 0.024 N.

6A, demonstrates the likeness of the trends clearly. The key assumption here, following from Chang et al.,⁶ is the uniqueness of the adhesion force for a given surface separation.

Figure 6B illustrates the relation between adhesion and roughness for a different batch of surfaces, prepared separately from, and in no obviously different manner than, the surfaces used in the experiments for Figure 6A. This set of experiments involved three different contacts to test a range of applied loads. For each fresh contact, a compressive load of either 0.024, 0.032, or 0.045 N was applied before relieving the stress and separating the surfaces. Deformations were measured, and adhesions were determined just as in Figure 6A. As can be seen in Figure 6B, applied loads of greater magnitude resulted in greater changes in roughness. Further, the variation of adhesion with roughness, or relative surface separation, is similar in form among all three contacts. Again, sliding the trends along the abscissa so they overlay illustrates this point, as shown by the inset in Figure 6B. The change in adhesion with roughness is consistent from contact to contact within a batch of surfaces while loads are applied.

The relation between adhesion and surface separation differs for the unloading process when asperity deformation is partially recovered, as compared to Figure 6A. The recovery behavior is marked in Figure 6B by the open symbols. This behavior is most apparent when larger loads are applied. The subtle difference between the loading and unloading process may result from a modest change in the roughness statistics due to the deformation of the asperities.

On a related note, our limited observations on subsequent recontact and repetition of the loading–unloading cycle show that the extent of hysteresis is lessened. Hysteresis is reduced, but not eliminated, since separation of the surfaces often results in some recovery of the asperity deformation. Hysteresis is, however, not observed when the surfaces are cycled without a separation event.

Though only contact between rough gold and smooth mica is considered here, the technique is sensitive to modest changes in surface free energy and/or surface preparations. The use of contact mechanics theory to relate measured deformations to adhesive behavior clearly highlights this difference, as illustrated by Figure 5A,B. The contacts represented in Figure 6A are between surfaces prepared separately from, and in no obviously different manner than, the surfaces studied for Figure 6B. All else remaining the same, the difference in behavior between the two batches of surfaces may be attributed to differing degrees of probable surface contamination. Even the measurement of adhesion between two mica surfaces is inconsistent, so this observation is not surprising.¹⁰ Nevertheless, the method described herein to determine the relation between adhesion and surface separation for rough contacts is self-consistent for the two surfaces in question and is quite sensitive to subtle changes in surface free energies.

Furthermore, the sensitivity of the method also provides a prediction of the relative adhesiveness between surfaces upon contact. The ability to resolve the contact area in these experiments allows comparison to predictions made by eq 4 at negligible (or zero) load. Systems which initially contact with a diameter greater than the one predicted by Greenwood and Tripp²⁵ are strongly adherent, as illustrated by Figure 5A, whereas systems which contact with a diameter equal to or less than the apparent contact diameter predicted by eq 4 tend to be weakly adherent or nonadherent, as illustrated by Figure 5B. The contact diameter of the system represented by Figure 5A at negligible load is nearly 120% greater than the predicted diameter for its nonadhesive counterpart. On the other hand, the contact diameter of the system represented by Figure 5B differs only 3% from the diameter predicted by Greenwood and Tripp for nonadhesive, rough contact at negligible load. This difference is reflected starkly in the measured pull-off forces, where the pull-off force measured between the surfaces represented by Figure 5A is nearly 5 times greater than the pull-off force measured between the surfaces represented by Figure 5B, even though the surfaces of Figure 5B experienced 0.008 N more force. These observations support the notion that initial contact may be nonadhesive due to surface roughness, but the system becomes more adhesive as asperities deform, allowing van der Waals forces to exert greater influence as the bodies draw nearer.

Last, our application of JKR theory to adhesive contacts between rough surfaces may also provide an opportunity to finally compare experimental measurements with detailed computational models. For example, Chang et al.⁶ determined how an adherence force, due to the fundamental work of adhesion, varied with relative surface separation for rough surfaces contacting in a flat plate geometry. Our method shows how adhesion strength, in the form of a pull-off force, varies with relative surface separation for a sphere-flat contact geometry. Though we do not undertake the task here, the simulation and experiment may be related to one another.

Conclusion

Deformations at the interface and in the bulk occur when rough, curved solids contact due to applied loads and surface

forces. The surface forces apparatus offers an ideal means of monitoring these changes with controlled, applied loads. To this end, contact and adhesion between molecularly smooth mica and microscopically rough gold is considered. This paper details how adhesion in this system varies when a multiple of metallic asperities contact and deform under external stress.

The lack of theory or simulation describing contact between rough, adhesive surfaces in a sphere against flat geometry led us to recall theories devised for ideal systems. Calling upon JKR theory to interpret the contact mechanics of our rough, adhesive systems illustrates two points. First, distinguishing whether a system is rough and nonadhesive, or smooth and adhesive, upon first contact is difficult; in both instances, a finite contact area results under negligible load. For one system in this study, the finite contact area corresponded to one predicted by Greenwood and Tripp²⁵ for nonadhesive contact for our particular surface (or roughness) statistic. Second, both theories suggest similar bulk deformation behavior. The contact mechanics approach quickly reveals, however, the adhesive nature of the rough system; a finite tensile load is required to separate the two bodies.

Applying JKR theory as an interpretive tool leads us to conclude that the bulk deforms in a manner whereby adhesion between the bodies effectively increases with increasing load. Concurrent deformations at the interface intuitively support this assertion; asperities deform, and surfaces draw nearer, thus abetting greater van der Waals attractions. This assertion is strongly supported by the observations illustrated in Figures 4A and 5A, where the constancy of roughness is matched by the constancy of the work of adhesion, as determined by JKR theory, upon separation of the surfaces. This way of viewing bulk and interfacial deformations allows us to show how adhesion effectively changes with relative surface separation—a form adopted by theoreticians modeling this contact phenomenon. Moreover, the hysteresis observed upon loading and unloading the contacting surfaces is explained.

This technique also demonstrates its sensitivity to subtle changes in surface properties with regard to contact, deformation, and adhesion. While self-consistency is observed for multiple contacts on the surfaces prepared in the same batch, the contact behavior can change if a different set of surfaces is prepared. This deviation may result from different nucleation conditions for the gold films, or simply from the experimental limitation of not operating in a vacuum.

The sensitivity of this approach is also its power. The technique offers us a means of systematically investigating other factors affecting the strength of adhesion and structure of the interface, such as surface chemistry and humidity. The chemistry of self-assembling monolayers is well-established and well-suited for our model rough system. Control of humidity in an enclosed chamber is a well-known technique. Further detailed studies of contact between microscopically rough surfaces is critically important if technology on these tiny scales is to be exploited fully.

Acknowledgment. We gratefully acknowledge support for this work from the National Science Foundation (CTS-9423780).

Supporting Information Available: Further experimental details for the methods used. This material is available free of charge via the Internet at <http://pubs.acs.org>.

References and Notes

- (1) Israelachvili, J. N. *Intermolecular and Surface Forces*; Academic Press Inc.: London, 1985; p 296.
- (2) Johnson, K. L.; Kendall, K.; Roberts, A. D. Surface energy and the contact of elastic solids. *Proc. R. Soc. London A* **1971**, *324*, 301.

- (3) Kendall, K. Adhesion: Molecules and Mechanics. *Science* **1994**, *263*, 1720–1725.
- (4) Levins, J. M.; Vanderlick, T. K. Impact of Roughness of Reflective Films on the Application of Multiple Beam Interferometry. *J. Colloid Interface Sci.* **1993**, *158*, 223.
- (5) Knarr, R. F.; Quon, R. A.; Vanderlick, T. K. Direct Force Measurements at the Smooth Gold/Mica Interface. *Langmuir* **1998**, *14* (22), 6414–6418.
- (6) Chang, W. R.; Etison, I.; Bogy, D. B. Adhesion Model for Metallic Rough Surfaces. *Trans. ASME* **1988**, *110*, 50–56.
- (7) Chowdhury, S. K. R.; Ghosh, P. Adhesion and Adhesion Friction at the Contact Between Solids. *Wear* **1994**, *174*, 9–19.
- (8) Chaudhury, M. K.; Whitesides, G. M. Direct Measurement of Interfacial Interactions between Semispherical Lenses and Flat Sheets of Poly(dimethylsiloxane) and Their Chemical Derivatives. *Langmuir* **1991**, *7*, 1013–1025.
- (9) Falsafi, A.; Deprez, P.; Bates, F. S.; Tirrell, M. Direct measurement of adhesion between viscoelastic polymers: A contact mechanical approach. *J. Rheol.* **1997**, *41* (6), 1349–1364.
- (10) Christenson, H. K. Adhesion and Surface Energy of Mica in Air and Water. *J. Phys. Chem.* **1993**, *97*, 12034–12041.
- (11) Horn, R. G.; Israelachvili, J. N.; Pribac, F. Measurement of the Deformation and Adhesion of Solids in Contact. *J. Colloid Interface Sci.* **1987**, *115*, 480–492.
- (12) Pollock, H. M.; Shufflebottom, P.; Skinner, J. Contact Adhesion Between Solids in Vacuum: I. Single-Asperity Experiments. *J. Phys. D: Appl. Phys.* **1977**, *10*, 127–138.
- (13) Chowdhury, S. K. R.; Pollock, H. M. Adhesion Between Metal Surfaces: The Effect of Surface Roughness. *Wear* **1981**, *66*, 307–321.
- (14) Maugis, D. P.; Pollock, H. M. Adhesion between Metal Surfaces: Surface Forces, Deformation and Adherence at Metal Microcontacts. *Acta Metall.* **1984**, *32* (9), 1323–1334.
- (15) Fuller, K. N. G.; Tabor, D. The Effect of Surface Roughness on the Adhesion of Elastic Solids. *Proc. R. Soc. London A.* **1975**, *345*, 327–342.
- (16) Gane, N.; Pfaelzer, P. F.; Tabor, D. Adhesion Between Clean Surfaces at Light Loads. *Proc. R. Soc. London A.* **1974**, *340*, 495–517.
- (17) McFarlane, J. S.; Tabor, D. Adhesion of Solids and the Effect of Surface Films. *Proc. R. Soc. A* **1950**, *202*, 224.
- (18) Levins, J. M.; Vanderlick, T. K. Reduction of the Roughness of Silver Films by the Controlled Application of Surface Forces. *J. Phys. Chem.* **1992**, *96*, 10405.
- (19) Tabor, D.; Winterton, R. H. S. The direct measurement of normal and retarded van der Waals forces. *Proc. R. Soc. London A* **1969**, *312*, 435.
- (20) Israelachvili, J. N.; Adams, G. E. Measurement of Forces between Two Mica Surfaces in Aqueous Electrolyte Solutions in the Range 0–100 nm. *J. Chem. Soc., Faraday Trans. 1*, **1978**, *74*, 975.
- (21) Tolansky, S., *Multiple-Beam Interferometry of Surfaces and Films*. Oxford University Press: London, 1948.
- (22) Levins, J. M.; Vanderlick, T. K. Impact of Roughness on the Deformation and Adhesion of a Rough Metal and Smooth Mica in Contact. *J. Phys. Chem.* **1995**, *99*, 5067–5076.
- (23) Hertz, H., Ed. *On the contact of elastic solids*; Miscellaneous Papers by H. Hertz; Schott, J. A., Ed.; Macmillan: London, 1882.
- (24) Greenwood, J. A.; Williamson, J. B. P. Contact of Nominally Flat Surfaces. *Proc. Royal Soc. (London), A* **1966**, *290*, 300–319.
- (25) Greenwood, J. A.; Tripp, J. H. The Elastic Contact of Rough Spheres. *J. Appl. Mech.* **1967** (March): p 153–159.
- (26) Vanderlick, T. K.; Scriven, L. E.; Davis, H. T. Forces between solid surfaces in binary solutions. *Colloids Surf.* **1991**, *52*, 9.
- (27) Levins, J. M.; Vanderlick, T. K. Extended Spectral Analysis of Multiple Beam Interferometry: A Technique To Study Metallic Films in the Surface Forces Apparatus. *Langmuir* **1994**, *10*, 2389–2394.
- (28) Levins, J. L.; Vanderlick, T. K. Characterization of the Interface between a Rough Metal and Smooth Mica in Contact. *J. Colloid Interface Sci.* **1997**, *185*, 449.
- (29) Levins, J. M. Contact and Adhesion Between Solids: Impact of Roughness and Surface Chemistry as Probed with a New Technique. In *Chemical Engineering*; University of Pennsylvania: Philadelphia, 1994; p 145.
- (30) Israelachvili, J. N. Thin Film Studies Using Multiple-Beam Interferometry. *J. Colloid Interface Sci.* **1973**, *44*, 259.
- (31) Thomas, T. R., Ed. *Rough Surfaces*, 1st ed.; 1982, Longman Group Limited: Harlow, 1982; p 261.
- (32) Frantz, P.; et al. Use of capacitance to measure surface forces 0.2. Application to the study of contact mechanics. *Langmuir* **1997**, *13*, 5957–5961.